Environ Sci Pollut Res (2017) 24:13808–13822
DOI 10.1007/s11356-017-8949-x

RESEARCH ARTICLE

The photocatalytic degradation of carbofuran and Furadan 35-ST: the influence of inert ingredients

Anđelka Tomašević[1] · Dušan Mijin[2] · Aleksandar Marinković[2] · Marina Radišić[3] · Nevena Prlainović[3] · Rada Đurović-Pejčev[1] · Slavica Gašić[1]

Received: 10 January 2017 / Accepted: 27 March 2017 / Published online: 12 April 2017

Abstract A comparative study on photocatalytic degradation of the pesticide carbofuran and its commercial product Furadan 35-ST in an aqueous suspension of ZnO, irradiated by long-wave light (315–400 nm), is presented in this study. In order to assess the effects of inert ingredients present in the commercial product Furadan 35-ST, non-competitive and competitive adsorption and kinetic studies of carbofuran degradation processes were conducted. A higher photochemical degradation rate was found for pure carbofuran in comparison to a two-component system, carbofuran and single addition of ingredients at appropriate concentrations, and the commercial product Furadan 35-ST. The overall effect of inert ingredients was evaluated from a competitive study using the model system of Furadan 35-ST. The results of a mineralization study, obtained by ion chromatography (IC) and total organic carbon (TOC) analyses, revealed the formation of acetate, oxalate, and formate ions. Photodegradation products of carbofuran, three of them detected for the first time, were identified based on high-performance liquid chromatography-tandem mass spectrometry (HPLC-MS/MS) and gas chromatography-mass spectrometry (GC-MS) results, and their photodegradation pathways were proposed.

Keywords Heterogeneous photocatalysis · Carbofuran · Furadan 35-ST · Inert ingredients · Transformation products

Responsible editor: Suresh Pillai

Electronic supplementary material The online version of this article (doi:10.1007/s11356-017-8949-x) contains supplementary material, which is available to authorized users.

✉ Nevena Prlainović
nprlainovic@tmf.bg.ac.rs

[1] Institute of Pesticides and Environmental Protection, Banatska 31b, P.O. Box 163, Zemun, Belgrade 11080, Serbia

[2] Faculty of Technology and Metallurgy, University of Belgrade, Karnegijeva 4, P.O. Box 3503, Belgrade 11120, Serbia

[3] Innovation Center, Faculty of Technology and Metallurgy, University of Belgrade, Karnegijeva 4, Belgrade 11120, Serbia

Introduction

The problem of water pollution with pesticides has been an environmental concern for many years (Konstantinou et al. 2004; Senthilnathan and Philip 2010; Ahmed et al. 2011). Pesticides as an integral part of modern agriculture are a very important class of water contaminants. Among various methods proposed for the removal of pesticides, the process of heterogeneous photocatalytic degradation has been suggested as an attractive way of treating contaminated water due to its cost-effective and non-toxic nature (Tomašević et al. 2010a; Tomašević et al. 2010b; Tomašević et al. 2014; Quiroz et al. 2011; Sharma and Lee 2016).

Carbofuran, $C_{12}H_{15}NO_3$, IUPAC name 2,3-dihydro-2,2-dimethylbenzofuran-7-ylmethylcarbamate, belongs to a large group of carbamate pesticides widely used in agriculture and with relatively good solubility in water (Tomašević and Gašić 2012) and a resulting great potential for groundwater and surface water contamination. Carbofuran is degraded in water by hydrolysis, microbial decomposition, and photolysis (MacBean 2012). It has been banned in the EU because of its potential adverse effects, e.g., acting as potential endocrine disrupter (Reg. EC No 1107/2009), but it is still in use in Africa and Asia (Otieno et al. 2010; Benicha et al. 2013; Farahani et al. 2007; Chowdhury et al. 2012; Cid et al. 2014). According to the Environmental Protection Agency, World Health Organization, and European Commission, carbofuran is a highly toxic compound. As an active acetylcholinesterase inhibitor, carbofuran is very toxic to mammals and fish. It

can produce extensive negative effects in aqueous ecosystems (MacBean 2012; EPA 2006).

Before application, pesticide active ingredients are formulated and put on the market as chemically different commercial products. Pesticide formulations are mixtures of active ingredient(s) and various inert ingredients, such as surfactants, solvents, antifoam compounds, and antifreeze compounds (Knowles 2005, 2008). Having in mind that such commercial products enter the environment during application, it seems very important to investigate and compare the degradation efficiency of an active compound itself and in the presence of inert ingredients used in commercial products. A number of studies have examined the influence of surfactants on the efficiency of pesticide degradation (Tanaka et al. 1977; Tanaka et al. 1979, 1981; Bianco Prevot et al. 1999; Arias et al. 2005; Kong and Lemley 2007; Sinha et al. 2009). Also, photodegradation of active ingredients has been a topic of many published papers and some of them related to degradation of commercially formulated products (Huston and Pignatello 1999; Malato et al. 2000; Lhomme et al. 2008; Ballesteros Martín et al. 2009; Colina-Márquez et al. 2009; Navarro et al. 2009; Zapata et al. 2009a, 2009b; Mazille et al. 2010; Vicente et al. 2014).

Various catalysts are known to be used during heterogeneous photocatalysis, such as TiO_2, ZnO, Fe_2O_3, MnO_2, CdS, and ZnS. Among them, TiO_2 was found the most effective (Daneshvar et al. 2003, 2004). Besides TiO_2, ZnO has also been frequently used. In comparison to TiO_2, ZnO absorbs over a larger fraction of the UV spectrum with threshold wavelength of 440 nm (Malato et al. 2009) or 425 nm (Behnajady et al. 2006). ZnO catalyst has a similar band gap energy (3.2 eV) as TiO_2 (~3.1 eV) and similar photocatalytic capacity (Malato et al. 2009). In addition, photocatalytic degradation with ZnO is more effective in acidic than in alkaline media (Daneshvar et al. 2004) because photodecomposition and photocorrosion of ZnO occur in alkaline media (Daneshvar et al. 2004; Daneshvar et al. 2007). It was reported that during photocatalytic degradation of the herbicide clopyralid in water, ZnO Merck was a better catalyst than TiO_2 P-25 (Evonik) (Berberidou et al. 2016). Also, Evgenidou et al. (2005) have reported that ZnO appeared to be the more efficient catalyst in comparison to TiO_2, especially at high concentrations (above 0.2 g L^{-1} of catalyst) (Evgenidou et al. 2005).

To the best of our knowledge, there are no reported studies relating to degradation of carbofuran and its commercial product Furadan 35-ST in the presence of ZnO catalyst or to the impact of inert ingredients on carbofuran photodegradation. Hence, the impact of six inert ingredients present in Furadan 35-ST formulation (Tensiofix CD001, Tensiofix CP002, propylene glycol, polyacrylic acid, xanthan gum, and Rhodamine B) on adsorption and photodegradation kinetics of carbofuran was examined comparatively.

Materials and methods

Materials

All chemicals used in the investigation were of reagent grade and were used without further purification. Hydrochloric acid, sodium carbonate, sodium hydrogen carbonate, sodium sulfate, and sodium hydroxide (all p.a.) were purchased from Merck. Analytical-grade carbofuran (99.5%) was granted by FMC, USA, while Furadan 35-ST was used as a commercial product (FMC, USA). Furadan 35-ST is a suspension concentrate for seed treatment (FS) and contains 344.4 g L^{-1} of carbofuran active ingredient (manufacturer data 350 g L^{-1}). The inert ingredients used in the investigation were Tensiofix CD001 and Tensiofix CP002 (S.A. Ajinomoto OmniChem N.V., Belgium), propylene glycol (PG) (Shell Chemicals Europe B.V., Netherlands), polyacrylic acid (Sigma-Aldrich), xanthan gum (Rhodia, Italy), and red color Rhodamine B (Riedel de Haën, Germany). The photocatalyst employed was a commercial ZnO obtained from Merck with surface area 10 m^2 g^{-1} and particle size 0.1–4.0 μm. HPLC-grade acetonitrile for HPLC analysis, methylene chloride for the extraction of carbofuran transformation products, and methanesulfonic acid for ion chromatographic analyses were provided by Fluka. All solutions were prepared with Millipore Waters deionized water (18.2 MΩ cm^{-1} at 25 °C).

The exact content of commercial pesticide formulations is usually a trade secret. Information on the composition of Furadan 35-ST type of formulation can be found in literature (Knowles 2005, 2006, 2008; Woods 2003). Typical formulations contain active ingredient (20–70%), wetting/dispersing agents (2–5%), antifreeze agent (5–10%), antisetting agent (0.2–2%), red color as a safety marker on dressed seed (0.1–2%), and water to 100%. After an additional qualitative/quantitative analysis of original preparation by LC and NMR analyses, the approximate content and class of inert ingredients were determined. Based on the results, a *model formulation (model system)* was prepared using the commercial ingredients of similar properties to the ones found in the original formulation, such as Tensiofix CD001 (1.8%) and Tensiofix CP002 (0.45%), which were used as wetting/dispersing agents. Other ingredients of the model formulation are the same as found in Furadan 35-ST, which are PG (5%) as antifreeze agent, xanthan gum (0.15%) and neutralized polyacrylic acid by triethanolamine (1.8%) as antisettling agents, and Rhodamine B (0.1%) as safety marker.

Photodegradation procedure

Solutions were prepared by dissolving carbofuran (and Furadan 35-ST) in deionized water, followed by additional degasification for 60 min in an ultrasonic bath. The initial concentration of carbofuran was 88.4 mg L^{-1} (4×10^{-4} M)

for both pure carbofuran and commercial Furadan 35-ST. The reactions were performed in an open glass thermostated reactor (cylindrical shape, volume 500.0 mL, 20 °C) with an 300-W Osram Ultra-Vitalux® lamp (UV-A:UV-B = 13.6:3 according to the manufacturer's specification) placed 300 mm from the surface of the reaction mixture. In a typical experiment, 250 mL of the carbofuran solution (or Furadan) and 2.0 g L^{-1} of catalyst were added. The pH-dependent carbofuran photodegradation study was performed at the following five different pH values: 2.7, 3.5, 5.9 (6.2), 9.6, and 10.2 with carbofuran concentration of 88.4 mg L^{-1}. The pH values of 5.9 and 6.2 were obtained by dissolution of pure carbofuran and Furadan 35-ST in deionized water, respectively. The pH values 2.7, 3.5, 9.6, and 10.2 of the carbofuran (and Furadan) solutions were adjusted before irradiation using 0.1 M HCl or NaOH. Before irradiation, the reaction mixture was stirred for 60 min in darkness in order to achieve adsorption equilibrium. Agitation was then applied (500 rpm) and solutions were subjected to irradiation for the next 120 min. At specific time intervals, appropriate samples of the suspension were withdrawn, centrifuged for 15 min, and filtered through a 0.20-μm Sartorius filter. Time-dependent determination of carbofuran concentration was performed using both UV/Vis and HPLC-UV methods. A water solution of pure carbofuran showed absorption peak at 275 nm, while water solution of Furadan 35-ST showed the following two absorption peaks: at 275 and 555.0 nm (Fig. S1). The second absorption peak originates from the red color of Rhodamine B dye.

Photodegradation procedures, designed to analyze the influence of the inert ingredients on the photodegradation rate of carbofuran in non-competitive and competitive conditions, were performed in three sets of photodegradation experiments (Fig. 1):

Set I: Non-competitive adsorption and kinetics of pure carbofuran,

Set II: Competitive adsorption and kinetics of carbofuran in a two-component system—carbofuran and one selected inert ingredient used at concentrations found in Furadan 35-ST, and

Set III: Competitive adsorption and kinetic photodegradation of carbofuran with all inert ingredients added—comparison of photodegradation rate of Furadan 35-ST and model formulation. The results of adsorption and kinetics study of pure carbofuran were used as the reference.

Analytical procedures

For UV/Vis spectrophotometric determination during photodegradation of carbofuran and Furadan 35-ST, the spectra were recorded on a Shimadzu 1700 UV/Vis spectrophotometer in a wavelength range from 200 to 600 nm. Due to the linear dependence between the initial concentration of carbofuran and absorption of carbofuran at 275 nm, the kinetics of degradation was monitored at 275 nm. The solution was used in amounts of 5.0 mL of all samples, and all UV/Vis and

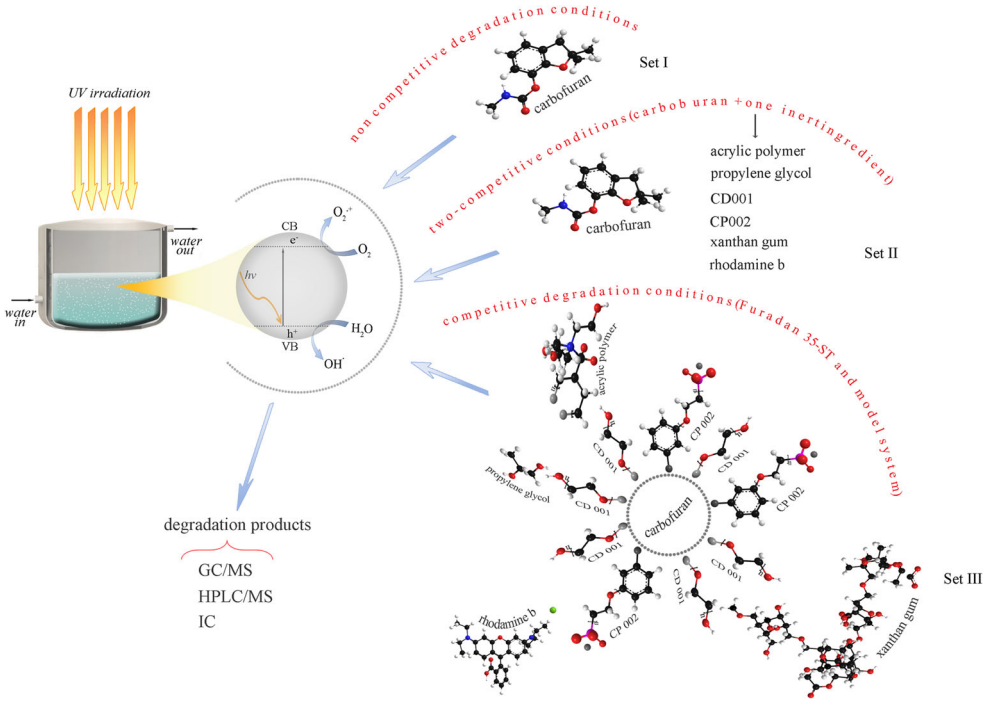

Fig. 1 Schematic presentation of non-competitive and competitive photodegradation conditions

HPLC-UV results were obtained as mean values from three determinations. HPLC-UV analysis was conducted at 280 nm at the ambient temperature (25 °C) on a Hewlett Packard HP 1050 liquid chromatography with a UV/Vis detector, equipped with a reversed-phase, column-type Zorbax Eclipse XDB-C18 150 × 4.6 mm (i.d.) × 5 μm. The mobile phase (flow rate 1.5 mL min^{-1}) was a mixture of methanol and water (70:30, *v*/*v*), and both samples and standards were diluted with methanol. Under the above chromatographic conditions, concentrations of carbofuran were determined from the peak area at retention time t_R = 1.63 min. The pH of the samples was adjusted by adding NaOH or HCl solutions (0.1 M). For ion chromatographic determinations, all carbofuran and Furadan 35-ST solutions were diluted and were filtered through Milex-GV 0.22-μm membrane filters and analyzed on a Dionex DX-300 ion chromatograph at ambient temperature (25 °C) with a suppressed conductivity detector. Ion chromatograph was equipped with a Dionex IonPac AS 14 column 250 × 4.0 mm (i.d.) for anion determination and Dionex IonPac CS12 column 250 × 4.0 mm (i.d.) for cation determination. The mobile phase for anion determination was a carbonate/bicarbonate mixture (3.5 mmol L^{-1} Na_2CO_3 + 1.0 mmol L^{-1} $NaHCO_3$), flow rate 1.0 mL min^{-1}, while for cation determination, it was a solution of methanesulfonic acid (20.0 mmol L^{-1}), flow rate 1.0 mL min^{-1}. The sample injection volumes were 50 μL for both anion and cation measurements. Prior to sample measurements, blank samples of deionized water were analyzed. Retention times for acetate, formate, nitrite, nitrate, and oxalate ions were 4.40, 4.80, 9.70, 10.20, and 21.50 min, respectively. Retention times for ammonium and methylamine ions were 4.25 and 4.40 min, respectively. For total organic carbon (TOC) analysis, the samples were analyzed on a Zellweger LabTOC 2100 instrument using high-temperature combustion followed by infrared CO_2 detection.

After photodegradation of carbofuran (and Furadan 35-ST), to extract the intermediates, 5 mL of irradiated carbofuran solution was withdrawn and extracted twice with methylene chloride (10 mL the first time and 5 mL the second). After separation from the aqueous solution, methylene chloride phase was dried with anhydrous sodium sulfate and concentrated to dryness using rotary vacuum evaporation. The residue was dissolved in 1 mL of methylene chloride, and an aliquot was analyzed by GC-MS in a Varian CP-3800 gas chromatograph equipped with a Saturn 2200 mass spectrometer as a detection device. A Varian VF 5-ms capillary column (30 m × 0.25 mm × 0.25 μm) and helium (1 mL min^{-1}) as the carrier gas were used. The oven temperature was programmed as follows: initially held at 80 °C for 5 min, then increased from 80 to 210 °C at a speed of 10 °C min^{-1} and held for 8.5 min, then increased from 210 to 300 °C at a speed of 30 °C min^{-1}, and finally kept at 300 °C for 2 min. The samples were analyzed in the splitless mode. The ion trap mass spectrometer was operated in the full-scan electron impact mode. The ion trap and transfer line temperatures were set to 220 and 250 °C, respectively.

An HPLC-MS analysis of photodegradation samples was also conducted. The HPLC–MS system consisted of a Thermo Fisher Scientific (Waltham, MA, USA) apparatus including a vacuum solvent degassing unit, quaternary pump (Surveyor), LTQ XL mass spectrometer with liner ion trap (Thermo Scientific, USA) with electrospray interface, and Xcalibur v.2.1 software package. Chromatographic separation was performed on the reversed-phase Zorbax Eclipse® XDB-C18 column, 75 × 4.6 mm (i.d.) × 3.5 μm (Agilent Technologies, Santa Clara, CA, USA). Chromatographic analysis was carried out using gradient elution, and the mobile phase consisted of water (A), methanol (B), and 10% acetic acid (C). For carbofuran and Furadan 35-ST analyses, the gradient changed as follows: 0 min, B 30%, C 1%; 30 min, B 100%; and 35 min, B 100%. The initial conditions were re-established and held for 10 min. An aliquot of 10 μL of each photodegradation sample was injected into the HPLC system. The analysis was conducted in the positive electrospray mode. The optimal source working parameters were as follows: source voltage (5 kV), sheath gas (32 au, i.e., 32 arbitrary units), auxiliary gas (8 au), and capillary temperature (350 °C). In the first step of the HPLC-MS analysis, full MS spectra were recorded in the range of 50–600 *m*/*z*. MS/MS analysis was conducted for most abundant ions by repeated injection of the sample.

Statistical analysis

All experiments were run in triplicates and the presented results are mean values from three determinations. Relative standard deviations were less than 3%.

Results and discussion

Photocatalytic degradation of pesticides depends on different operational parameters, such as pH, initial concentration, photocatalyst properties and concentration, temperature, light intensity, and the pollutant properties in a non-competitive condition. In a competitive condition, the influence of another reacting species must be additionally considered. Selection of the most influential factor to carbofuran photodegradation process was the main task of the presented study. The effect of ZnO catalyst concentration was evaluated in a previous work (Tomašević et al. 2007; Tomašević 2011), and the concentration of 2 g L^{-1} was again used in this study based on those results. Although MacBean observed degradation of carbofuran during photolysis (MacBean 2012), Tomašević detected no appreciable extent of it (Tomašević 2011). The difference in results could be attributed to different experimental conditions, e.g., use of natural and deionized water.

Effect of the initial pH on photodegradation

The interpretation of pH effects on the efficiency of photodegradation process is a challenging and complex task due to many related process parameters affecting the photodegradation rate/mechanism. The effect of solution pH on oxidation of organic compounds is an important element of the analysis due to its essential influence on the generation of hydroxyl radicals, i.e., photogeneration of electron-hole pairs at the surface of photocatalyst particles (Tomašević et al. 2010a, 2010b, 2014; Daneshvar et al. 2004, 2007; Neppolian et al. 2002a). The following three possible reaction mechanisms can contribute to pesticide degradation: destruction/consumption by $OH^{\cdot}$ radical or some other oxidative species, oxidation by the generated positive hole, and reduction by the generated electron in conduction band. Moreover, the solution pH controls the properties of electrical double layer at solid/solution interface and protonation/deprotonation processes in the course of a photodegradation process. The point of zero charge (pH_{PZC}) value of ZnO surface is 9.0 ± 0.3 (Daneshvar et al. 2007), which indicates that surface charge density is negative at pH higher than 9.0. It means that a catalyst could achieve electrostatic attraction/repulsion with the species generated in the course of photodegradation process at different extents at operating pH. At pH > pH_{PZC}, intensive interaction with positively charged species is significant, and in that sense, it was necessary to perform a photocatalytic study at different initial pH.

The results of our kinetic study at different initial pH, 2.7, 3.5, and 5.9 for carbofuran (or 6.2 for Furadan 35-ST), 9.6 and 10.2, after processing, by determination of pseudo-first-order rate constant k, Eq. (S3), and half-life time, Eq. (S5), are given in Fig. S2 and Table 1. The obtained results imply that the reaction proceeds faster in acidic media for both carbofuran and Furadan 35-ST, and the initial photodegradation rates followed a decreasing trend with increasing pH (Fig. S2). In the acidic media (pH 2.7 and 3.5), the 1.4 times higher degradation rate of carbofuran versus carbofuran in Furadan 35-ST was attributed to the interference of inert ingredients. Electrostatic attraction is greater in the acidic pH; i.e., the increased attraction of electron density at phenyl ring and carbamate group of carbofuran and positive ZnO surface contributes to an increased degradation rate in the acidic media.

Table 1 Pseudo-first-order rate constants of carbofuran and Furadan 35-ST at different pH and correlation coefficients

Investigated system	pH	k (min^{-1})	R^2
Carbofuran	2.7	0.1497	0.9890
Furadan 35-ST		0.1047	0.9904
Carbofuran	3.5	0.1302	0.9654
Furadan 35-ST		0.0994	0.9888
Carbofuran	5.9	0.1072	0.9836
Furadan 35-ST	6.2	0.0889	0.9638
Carbofuran	9.6	0.0810	0.9584
Furadan 35-ST		0.0737	0.9463
Carbofuran	10.2	0.0724	0.9786
Furadan 35-ST		0.0710	0.9498

By increasing pH to 5.9 or 6.2, attractive interactions became weaker, and the degradation rate thus lower, while a 1.2 times higher k, 0.1072 versus 0.0889 min^{-1}, was obtained for carbofuran in relation to Furadan 35-ST, respectively. At pH 9.6, the degradation rate of pure carbofuran showed a decreasing trend, and the k for pure carbofuran was 1.1 times higher than for Furadan 35-ST (Table 1). At pH 10.2, the two rate constants were similar. It could be expected that hydroxyl ions participate in the hydrolytic reaction of the carbamate group, contributing to the increase of degradation rate. Additionally, due to its amphoteric nature, ZnO can undergo a significant dissolution at higher pH (Daneshvar et al. 2008; Comparelli et al. 2005), forming water-soluble basic tetrahydroxozincate ion. This ion is diffusionally transported to the bulk of the solution, oppositely to carbofuran transport, and contributes to increased carbofuran desorption and decrease of the degradation rate is a consequence.

Among other factors, the difference in photodegradation rates could also be attributed to the effect of aggregations/micelle formation in a suspension that contributes to inhibition of a photodegradation process. The solubilization of active compounds by micelle formation had been previously discussed (Tanaka et al. 1981; Kong and Lemley 2007; Sinha et al. 2009; Zhang et al. 2012; Tang et al. 2016). Carbofuran is hardly soluble in water (0.320 g L^{-1} at 20 °C), and most of the active compound is present in the core of formed micelles. Surfactants, wetting/dispersing agents, form micelles above the critical micelle concentration by aligning the hydrophobic groups to the inside and hydrophilic groups to the outside, being in contact with aqueous phase (Tadros 2005). As a result, the following three effects crucially determine the rate of photodegradation process: carbofuran diffusional transport from bulk and micelle and the competitive interaction of ingredients with the active species. Differences in diffusional transport of carbofuran from bulk solution and micelle-solubilized carbofuran could contribute to lower photodegradation rate. Surfactants present in the micelle shell could play a double role, which are slow down diffusional transport and could additionally be possible competitors for photogenerated active species. Our kinetic results (Table 1) confirmed that interactions/availability of carbofuran present in micelles, i.e., Furadan 35-ST, or "free" carbofuran reacting with active species at the catalyst surface are different. It is well known that photodegradation is a non-selective process which takes place with the most active group/moieties of approaching/adsorbed molecules. Competition between the active compound and inert ingredients in the adsorbed micelle

(admicelle), due to their structural differences, shows various degradation rates/routes. Also, the aromatic moiety in the structure of pesticides or surfactants may also act as a possible photosensitizer or active species quencher (Katagi 2004).

The pseudo-first-order rate constant of degradation reaction decreased from 0.1497 to 0.0724 min^{-1} for carbofuran and from 0.1047 to 0.0710 min^{-1} for Furadan 35-ST with the initial pH increase from 2.7 to 10.2, respectively. The presented results are consistent with previous findings regarding photodegradation with ZnO in acidic media (Daneshvar et al. 2004). It was explained by a contribution of the ZnO catalyst to photodecomposition and photocorrosion processes (Daneshvar et al. 2004, 2007; Neppolian et al. 2002a; Neppolian et al. 2002b) and by a probably increased electrostatic attraction between carbofuran and the more positive ZnO surface in acidic media.

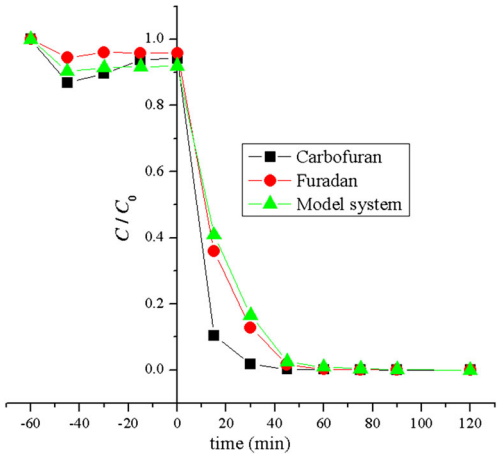

Fig. 2 Adsorption and photodegradation kinetics of carbofuran (pH 5.9), Furadan 35-ST, and model system (pH 6.2)

Adsorption versus degradation rate of carbofuran, Furadan 35-ST, and model system

In order to explain the effects of inert ingredients on adsorption and carbofuran photodegradation rate, the following three systems were studied in detail: carbofuran, Furadan 35-ST, and model system (Fig. 1). The effects of inert ingredients could be manifested by interference/slowing down of diffusional transport, adsorption/desorption, or competition in photodegradation processes through consumption of the active species or post-reaction of photodegradation species after desorption from the catalyst surface. Well-dispersed photocatalyst particles provide available surface active sites at the particle/solution interfaces, and thus, a high extent of pesticide adsorption and photodegradation provides a high extent of pollutant degradation. Adsorption precedes the photocatalytic process and thus affects carbofuran's approach to the photocatalytic surface and its photodegradation rate. In that sense, a comprehensive study on the influence of inert ingredients on adsorption and photodegradation of carbofuran was performed, and the results are presented in Fig. 2.

The results of the three-system adsorption studies of carbofuran revealed a slightly higher adsorption under non-competitive conditions regarding Furadan 35-ST, 5.8 versus 4.2%, respectively, while the highest adsorption was detected for the model formulation, 8.0% (Fig. 2). Somewhat higher adsorption of carbofuran in the system with model formulation, in comparison to Furadan 35-ST, indicated differences which originated from the properties of the components used in those two systems, but regardless of this fact, the presented results provide a reliable methodology which could be applied for studying other commercial products. Among the used inert ingredients, polyacrylate, xanthan gum, and propylene glycol showed the largest adsorption of 7.9, 7.5, and 6.2%, respectively, while the other ingredients showed less than 5% adsorption under non-competitive conditions.

Photocatalytic efficiency is determined by the time-dependent production of the active oxidative species, hydroxyl radical $OH^{\cdot}$, obtained in the reaction of holes and surface-bound water (Fig. 1). The consumption of active species by either carbofuran or inert ingredients was evaluated by performing competitive kinetic experiments, and determination of the structure of photodegradation products ("Mineralization study of carbofuran and Furadan 35-ST" section) provided a deeper insight into photodegradation pathways.

Differences in photodegradation rates, shown in Fig. 2, were significant for 15 min, which indicated a detrimental influence of the inert ingredients present in the reaction medium containing Furadan 35-ST. For the period of 15 min, the concentration of carbofuran decreased nearly 10 times (from 88.4 to 8.7 mg L^{-1}; 90% degraded), while in the case of Furadan 35-ST, carbofuran concentration decreased 2.9 times (from 88.4 to 30.4 mg L^{-1}; 70% degraded) compared to initial concentration. After 30 min of irradiation, 1.5 mg L^{-1} (98.3%) of pure carbofuran and 10.9 mg L^{-1} (87.7%) of carbofuran from Furadan 35-ST were detected. After 45 min of irradiation, 0.15% of carbofuran and 1.4% of carbofuran from Furadan 35-ST were detected, while carbofuran was not detected after 2 h. The k value was higher for carbofuran degradation, 0.1072 min^{-1}, than for Furadan 35-ST, 0.0889 min^{-1} (Table 1). A small difference found for Furadan 35-ST and the model system (Fig. 2) may be attributed to the influence of both properties of inert ingredients and the applied manufacturer production technology.

Effect of inert ingredients on photodegradation efficiency of carbofuran

Results of mutual contribution of all ingredients in Furadan 35-ST and model formulation on adsorption and

photodegradation rates are presented in the "Effect of the initial pH on photodegradation" and "Adsorption versus degradation rate of carbofuran, Furadan 35-ST, and model system" sections. In order to analyze effect of inert ingredients on adsorption and photodegradation rate of carbofuran, three sets (I–III) of adsorption and kinetic experiments were performed ("Photodegradation procedure" section).

In the first step, a non-competitive photodegradation study of carbofuran and inert ingredients was performed. No adequate analytical procedure has been established for measuring photodegradation rate of xanthan gum and polyacrylate. The apparent k values for the selected ingredients were 0.0584 min^{-1} for PG, 0.0868 min^{-1} for Rhodamine B, 0.0296 min^{-1} for CP002, and 0.0842 min^{-1} for CD001. Inhibition efficiency could be evaluated from the determined k values, but more relevant results were obtained from the competitive study.

In a two-component system, carbofuran degradation was mostly inhibited by the addition of polyacrylate followed by PG and Rhodamine B (Fig. 3a and Table 2). The surfactants CP002 and CD001 exhibited low inhibitory effects. The surfactant molecules in admicelle adsorbed onto the ZnO surface could, via hydrogen bonding or electrostatic attraction, contribute to retardation/enhancement of adsorption/desorption of carbofuran/photodegradation products. A low enhancement of photodegradation was found in the presence of xanthan gum (Fig. 3b and Table 2). This result indicates that both the molecular interaction at catalyst/solution interface and ones operating in bulk solution contribute to repulsive/attractive interactions of carbofuran/ingredient and carbofuran/catalyst surface is reflected in a change of rate constant values. The largest differences in the photodegradation rates were found at the begging of the process, while no observable differences were noticed after 90 min.

Effect of salt concentration on carbofuran and Furadan 35-ST photodegradation

Inorganic salts, usually present in both surface and ground waters, could exhibit either beneficial or detrimental effect on the photocatalytic decomposition rate of pollutants. The presence of inorganic ions could block holes and $^{\bullet}OH$ radicals causing decrease in the degradation rate of pollutants (Behnajady et al. 2006; Neppolian et al. 2002b; Daneshvar et al. 2007). The presence of sulfate (Tamimi et al. 2006), carbonate (Behnajady et al. 2006; Neppolian et al. 2002b), chloride (Neppolian et al. 2002b; Tamimi et al. 2006), and nitrate ions (Tamimi et al. 2006) causes an appropriate decrease in photocatalytic degradation efficiency in relation to their ability to react as hydroxyl radical scavengers (Neppolian et al. 2002b; Wang et al. 2013).

The effect of interfering ions was investigated under competitive conditions using carbofuran (C_0 = 88.4 mg L^{-1}) and appropriate sodium salt of the counter ions of interest at the concentration usually found in natural water (0.1 and 0.5% *w/v*). The effect of sodium nitrate was studied only in the concentration of 0.1% due to the interference of nitrate ions and carbofuran absorption. The effect of sodium cation could be neglected, as it was previously reported by Mohammad et al. (1990), and thus, the overall salt effect was considered in relation to the counter anion used. The obtained results are presented in Table 3.

According to the results presented in Table 3 concerning carbofuran, all the used anions showed that sodium carbonate was the most powerful inhibitor, while chloride was the weakest. The ratios of degradation rate of carbofuran under non-competitive conditions, 0.1072 min^{-1}, and those obtained under competitive conditions using the salt concentration of 0.1% *w/v* were 35.7, 1.6, 1.4, and 1.2 times lower in the presence of CO_3^{-}, SO_4^{2-}, NO_3^{-}, and Cl^{-} ions, respectively. Somewhat lower rate constants were obtained using 0.5% of appropriate salts excluding carbonate ions (Table 3). With salt

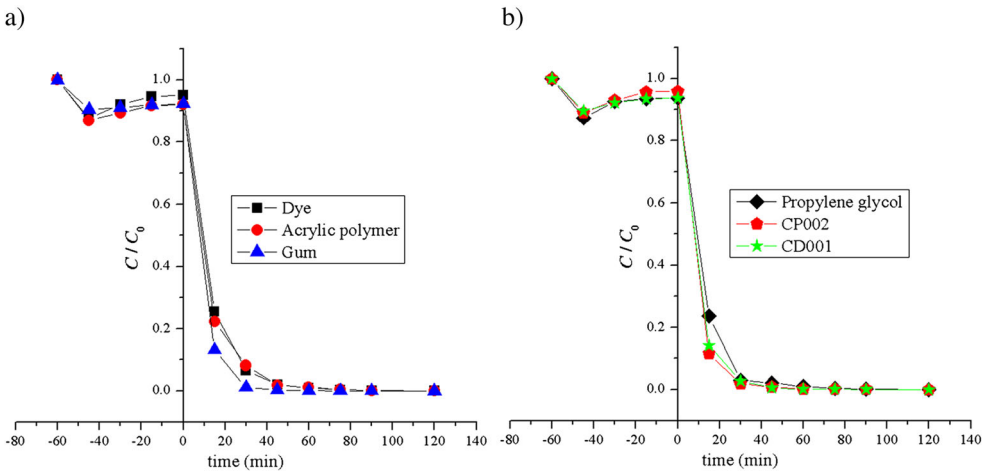

Fig. 3 Adsorption and photodegradation processes in a two-component system of carbofuran with **a** xanthan gum, polyacrylate, and Rhodamine B and **b** Tensiofix CP002 and CD001 and propylene glycol

Table 2 Pseudo-first-order rate constants of carbofuran photodegradation in a two-component system, Furadan 35-ST and model system, and correlation coefficients

Compound/ingredient	k (min^{-1})	R^2
Carbofuran	0.1072	0.984
Furadan 35-ST	0.0889	0.964
Carbofuran/Rhodamine B	0.0783	0.986
Carbofuran/propylene glycol	0.0782	0.945
Carbofuran/polyacrylic polymer	0.0764	0.983
Carbofuran/Tensiofix CP002	0.1018	0.954
Carbofuran/Tensiofix CD001	0.1042	0.970
Carbofuran/xanthan gum	0.1130	0.938
Model system (model formulation)	0.0741	0.986

concentrations of 0.1%, carbofuran in Furadan 35-ST degraded 80.8, 3.9, 3.7, and 7.9 times more slowly in the presence of CO_3^-, SO_4^{2-}, NO_3^-, and Cl^- ions, respectively (Table 3). Excluding carbonate ions, the decrease in rate constants was obtained using 0.5% of appropriate salts and Furadan formulation (Table 3).

Generally, it could be inferred that the photocatalytic degradation rate constant (k) of carbofuran with salt concentration of 0.1% *w/v* decreases in the following order: k (salt-free carbofuran solution) > k (Cl^-) > k (NO_3^-) > k (SO_4^{2-}) > k (CO_3^-), while the photocatalytic degradation rate constants for 0.5% *w/v* salt concentration have the same order (nitrate ions are not considered). The inert ingredients present in Furadan 35-ST formulation cause a change in the following rate constant order: k (Furadan 35-ST salt-free) > k (NO_3^-) > k (SO_4^{2-}) > k (Cl^-) > k (CO_3^-), which indicates a complex influence of the present ingredients, which participate in a side-reaction modifying/decreasing rate at which carbofuran is decomposed. Detailed discussion of the impact of each of the individual anions is given in Supplementary material ("Effect of salt concentration on carbofuran and Furadan 35-ST photodegradation" section).

Mineralization study of carbofuran and Furadan 35-ST

In order to get a deeper insight into photodegradation mechanism, a mineralization study of carbofuran and Furadan 35-ST was performed using ion chromatography (IC) and TOC analyses. Photocatalytic degradation of carbofuran had been investigated earlier using different photoprocesses, and the presence of several inorganic ions in reaction solutions was confirmed (Huston and Pignatello 1999; Tennakone et al. 1997; Katsumata et al. 2005; Mahalakshmi et al. 2007). On the other hand, no data are available about mineralization of any carbofuran-based commercial product in the presence of ZnO catalyst. Considering the structure of carbofuran, the formation of ammonia, nitrate, and nitrite ions could be expected as photodegradation products of carbofuran. Instead of that, oxalate, acetate, and formate ions were detected (Fig. 4a).

Figure 4a shows that the concentration of all ions originated from pure carbofuran increases over a period of 45 min, and after that gradually decreases. After 120 min, the concentration of acetate ions was highest, while the concentrations of oxalate and formate ions were similar. The concentrations of oxalate, formate, and acetate ions, obtained from Furadan 35-ST, were more than double those generated from carbofuran. The gradual increase in acetate and formate ion concentrations with time indicates that their formation is a result of degradation of both carbofuran and the ingredients present in Furadan 35-ST, such as polyacrylate and xanthan gum. For example, the concentration of acetate, produced by polyacrylate and xanthan gum photodegradation, was found to be 12 and 5 mg L^{-1} after 120 min, respectively, while the total concentration of acetate ions was 31.5 mg L^{-1}.

Generation of ions, which describes a time-dependent profile of formate, acetate, and oxalate ions (Fig. 4), was defined by single hydroxyl radical attack at either carbonyl carbon or α-position to keto group producing formate and acetate ions, respectively (Fig. S3). A concomitant formation of Mw 122 and 110 molecules could be supposed. Double hydroxyl radical attack caused a degradation of furan-3-on moiety to phenol and oxalate (Fig. S3). The degradation path which

Table 3 The effect of initial salt concentration on the photocatalytic degradation rate of carbofuran and Furadan 35-ST (C_0 = 88.4 mg L^{-1}, c(ZnO) = 2.0 g L^{-1}, pH 5.9 for carbofuran and 6.2 for Furadan)

Salt concentration (% *w/v*)		Rate constant, k (min^{-1})			
		CO_3^-	SO_4^{2-}	NO_3^-	Cl^-
0.1	Carbofuran	0.0030	0.0676	0.0756	0.0886
	Furadan 35-ST	0.0011	0.02241	0.0243	0.0113
0.5	Carbofuran	0.0080	0.0611	–	0.0691
	Furadan 35-ST	0.0015	0.0121	–	0.0091

Reference value of the rate of carbofuran degradation under non-competitive conditions 0.1072 min^{-1} and Furadan 35-ST 0.0889 min^{-1}

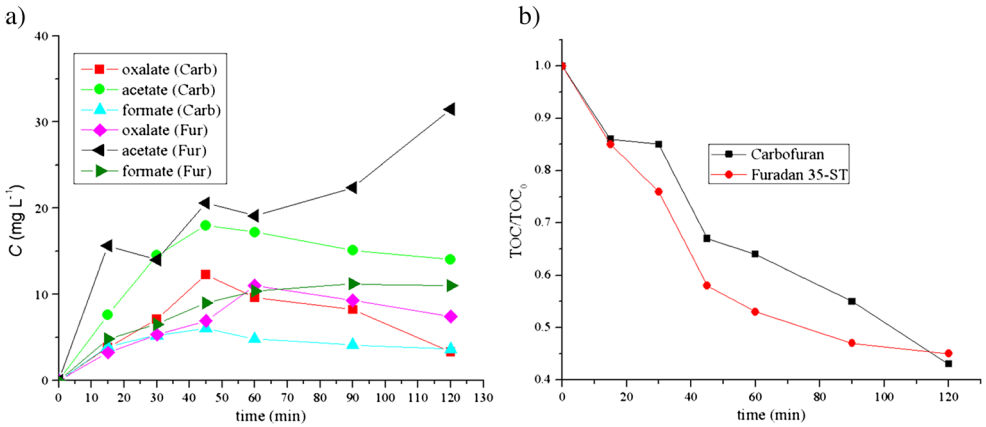

Fig. 4 Degradation and mineralization of carbofuran and Furadan 35-ST

produces acetate ions has the largest contribution, while formate formation is the process of lowest probability (Fig. S3).

Also, in the case of carbofuran and Furdan 35-ST, an IC analysis showed an appearance of methyl ammonium ion, $CH_3NH_3^+$. In our previous publication, related to methomyl photo-Fenton process (Tomašević et al. 2010a), it was demonstrated that methylamine was formed as a consequence of an incomplete photocatalytic-induced degradation process. Also, Oller et al. (2006) confirmed the formation of $CH_3NH_3^+$ during the photocatalytic degradation of several nitrogen-containing pesticides, which are dimethoate, cymoxanile, oxamyl, and methomyl (Oller et al. 2006).

Mineralization of organic carbon in both pure carbofuran and Furadan 35-ST was incomplete, 57 and 55%, respectively (Fig. 4b), although carbofuran was practically absent from the analyzed solutions (Fig. 2). Because of the fact that TOC elimination rates were not proportional to the rates of carbofuran disappearance in both pure carbofuran and Furadan 35-ST, a study on carbofuran transformation pathways was necessary.

Identification of photodegradation products—HPLC-MS/MS and GC-MS analyses

Photocatalytic degradation products obtained during irradiation of carbofuran and Furadan 35-ST were identified by using GC/MS and HPLC/MS^n techniques.

Pure carbofuran and Furadan 35-ST degradation using HPLC-MS analysis

Evaluation of degradation products for both carbofuran and Furadan 35-ST was based on the results obtained by HPLC-MS analysis. According to the HPLC-MS time-dependent monitoring of carbofuran photodegradation (Fig. 5a), a concomitant disappearance of carbofuran could be observed and the appearance of 2,2-dimethyl-2,3-dihydrobenzofuran-3,7-diol (3-hydroxycarbofuran) (t_R = 14.72 min) and 7-hydroxy-2,2-dimethylbenzofuran-3(2*H*)-one (3-ketocarbofuran phenol) (t_R = 17.26 min) (Fig. S4). A somewhat lower rate of carbofuran degradation in Furadan 35-ST was noticed (Fig. 5a), and carbofuran in both systems was completely decomposed after 60 min of irradiation. Over the same period, two products showed sharp peaks which disappeared simultaneously with carbofuran disappearance (Fig. 5). A significantly higher intensity of the 3-hydroxycrabofuran peak (Fig. 5b), compared to 3-ketocarbofuran phenol (Fig. 5c), indicates that the main process is hydroxyl attack at 3-position of furane ring. A similar profile of time-dependent concentration change of 3-ketocarbofuran phenol was found for carbofuran and Furadan 35-ST in a time period from 0 to 17.5 min. After that period, the concentration of 3-ketocarbofuran phenol steeply decreased to zero for carbofuran (42.5 min), while the decrease for Furadan 35-ST started after 30 min and complete disappearance was observed after 60 min (Fig. 5c). Lower degradation rate found for Furadan 35-ST indicates that the protective role of ingredients present in Furadan 35-ST lasted for ~30 min due to a competitive exhaustion of the generated oxidative species.

Fragmentation ions generated by carbofuran photodegradation are shown in Table 4; fragmentation paths in Figs. 5, 6, and 7; and HPLC/MS spectra in Fig. S4. The first photocatalytic degradation product, ion at *m*/*z* 238 identified as 3-hydroxycarbofuran, was reported earlier (Fenoll et al. 2013; Wang and Lemley 2003; Ying-Shih et al. 2009; Detomaso et al. 2005). The second photocatalytic degradation product, ion *m*/*z* 179 identified as 3-ketocarbofuran phenol, was also reported previously (Katsumata et al. 2005; Kuo et al. 2006; Li-An et al. 2011; Lopez-Alvarez et al. 2011; Fenoll et al. 2013; Wang and Lemley 2003; Ying-Shih et al. 2009).

The proposed fragmentation pathways of carbofuran, 3-hydroxycarbofuran and 3-ketocarbofuran phenol, and related fragmentation products are given in Fig. 6. An analysis of the MS spectrum of carbofuran (Fig. 6a) indicated that an appearance of the peak at *m*/*z* 165, attributed to carbofuran phenol, was due to a cleavage of the carbamate group from the parent compound. Loss of an allylic radical from *m*/*z* 165 produced 2,3-dihydroxybenzyl cation, an ion at *m*/*z* 123, which could be

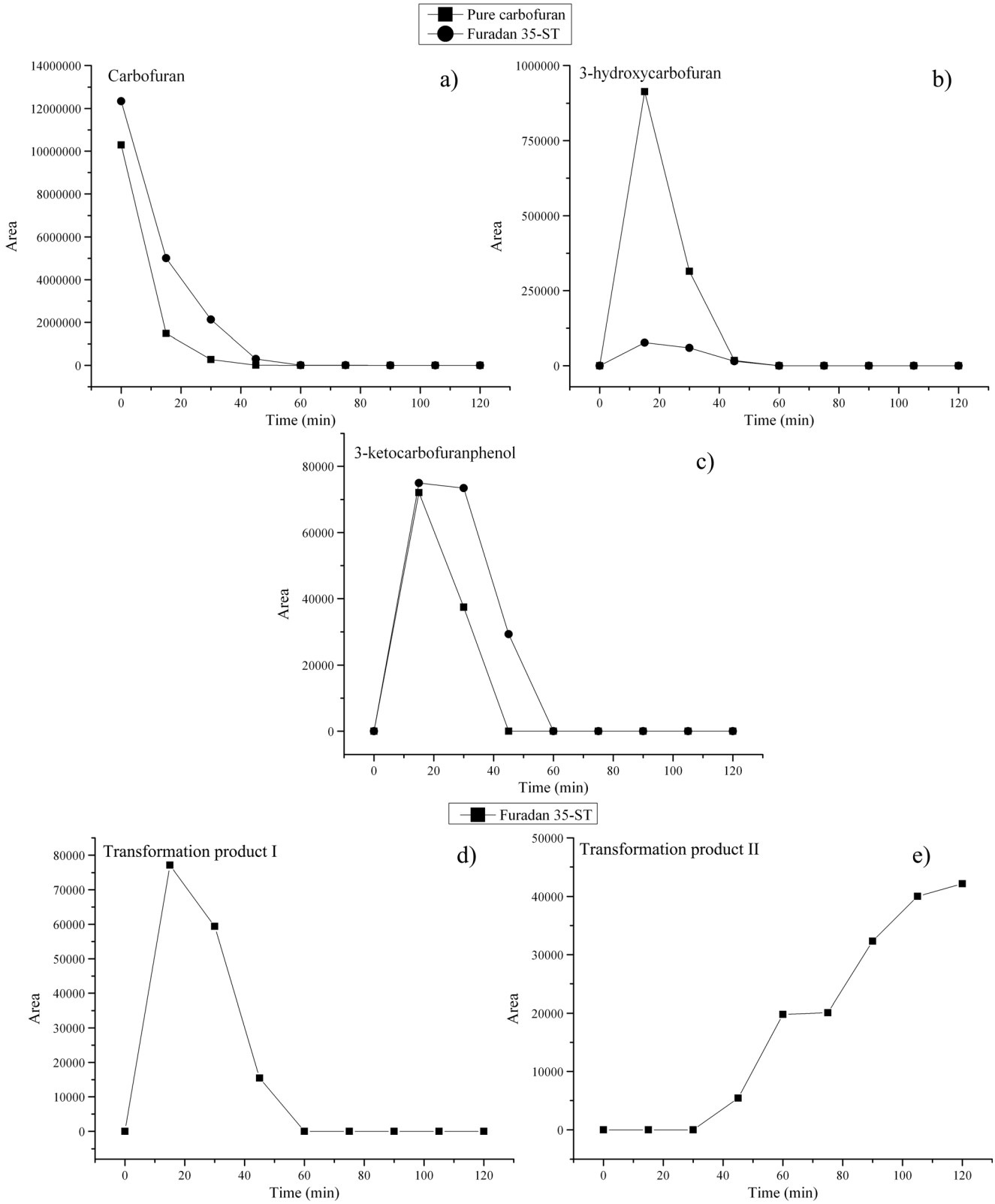

Fig. 5 Time-dependent profile generation in a photodegradation system of pure carbofuran and Furadan 35-ST. **a** Carbofuran. **b** 3-Hydroxycarbofuran. **c** 3-Ketocarbofuran phenol. **d** TP I. **e** TP II

presented by resonantly stabilized dihydroxy tropylium cation/radical. The ion at m/z 238 was identified as 3-hydroxycarbofuran (Fig. 6b). It was obtained in a course of photodegradation transformation by hydroxyl radical attack

Table 4 HPLC/MS and MS^2 data of selected precursor ions detected in photodegradation samples of carbofuran and Furadan 35-ST

Compound	Mw	MS, *m/z*	MS^2 (relative abundance), *m/z*	Carbofuran	Furadan 35-ST
Carbofuran	221	222 $[M + H]^+$, 244 $[M + Na]^+$	165 (100), 123 (5)	Detected	Detected
3-Hydroxycarbofuran	237	238 $[M + H]^+$, 260 $[M + Na]^+$	181 (100), 163 (10)	Detected	Detected
3-Ketocarbofuran phenol	178	179 $[M + H]^+$	161 (100), 151 (45), 179 (20)	Detected	Detected
Transformation product I (TP I)	239	240 $[M + H]^+$, 262 $[M + Na]^+$	222 (100), 180 (45), 194 (40), 165 (15), 240 (5)	Not detected	Detected
Transformation product II (TP II)	152	153 $[M + H]^+$	125 (100),135 (80), 111 (50), 153 (40), 95 (45), 144 (25)	Not detected	Detected

on benzylic hydrogen of carbofuran (3-position of furan ring). The fragmentation pathways of 3-hydroxycarbofuran is presented in Fig. 6b. The most abundant fragment, ion *m/z* 181, was obtained by methyl isocyanate removal forming protonated 3-hydroxy-carbofuran phenol. Characteristic fragmentation products, obtained by dehydration of *m/z* 181 ion, produced 7-hydroxy-2,2-dimethyl-2,3-dihydrobenzofuran-3-ylium ion found at *m/z* 163. A photodegradation product obtained from carbofuran by methyl isocyanate elimination in the first step, and followed by hydroxylation of benzylic hydrogen and oxidation produced 3-ketocarbofuran phenol, an ion found at *m/z* 179 (Fig. 6c). Two main fragmentation paths were found for this ion; dehydration produced 2,2-dimethylbenzofuran-3(2*H*)-one, an ion found at *m/z* 161, and the second one is elimination of carbon monoxide, which produced 2,2-dimethyl-2*H*-benzo[b]oxet-6-ol, *m/z* 151 ion.

From the MS spectra of Furadan 35-ST, besides the presented 3-hydroxycarbofuran and 3-ketocarbofuran phenol (Fig. 6), two additional transformation products were detected (Table 4). The first one, TP I, was obtained by hydroxylation of benzylic hydrogen at position 3 in the first step, and scission of etheral bond producing 3-(1,2-dihydroxy-2-methylpropyl)-phenylmethylcarbamate, an ion detected at *m/z* 240 (Fig. 7) (Detomaso et al. 2005). Transformation product I reaches maximum concentration after 17.5 min of photocatalytic reaction, while after 60 min, this peak completely disappeared (Fig. 5). The most intensive ion observed in MS^2 spectra, obtained by dehydration of *m/z* 240 ion (Table 4), was protonated carbofuran (ion at *m/z* 222). The identity of fragment ion at *m/z* 222 was confirmed by a subsequent MS^3 analysis, which produced characteristic fragment ions found in MS spectra of carbofuran (Fig. 5). Loss of a C_2H_6NO

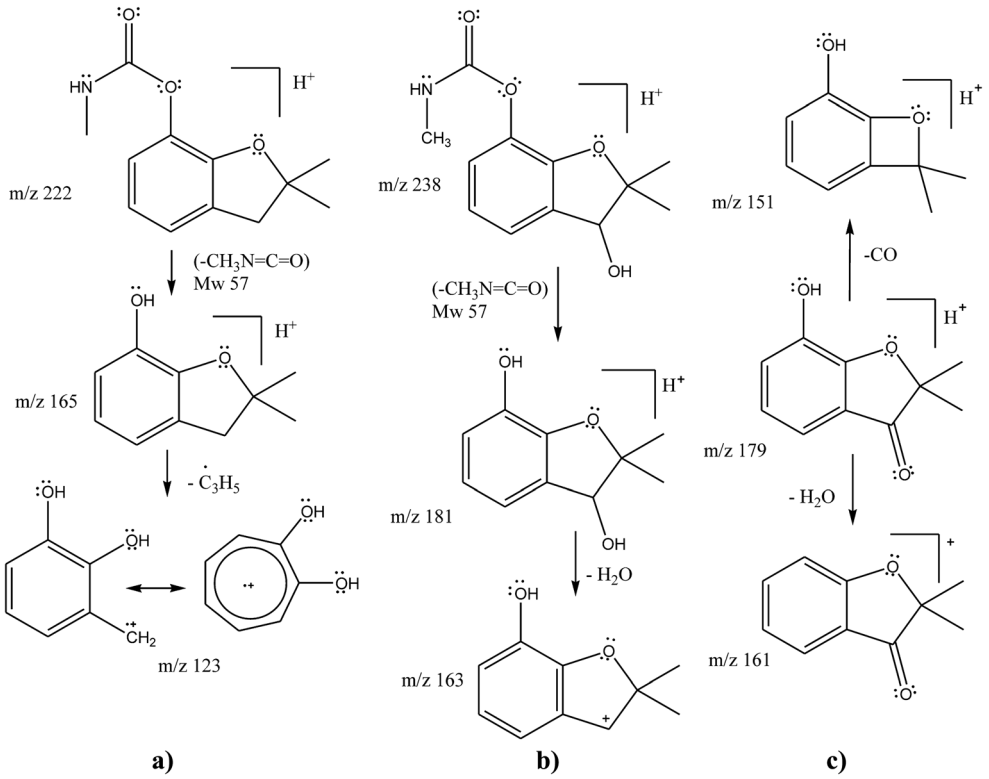

Fig. 6 Main fragmentation pathways of **a** carbofuran, **b** 3-hydroxycarbofuran, and **c** 3-ketocarbofuran phenol

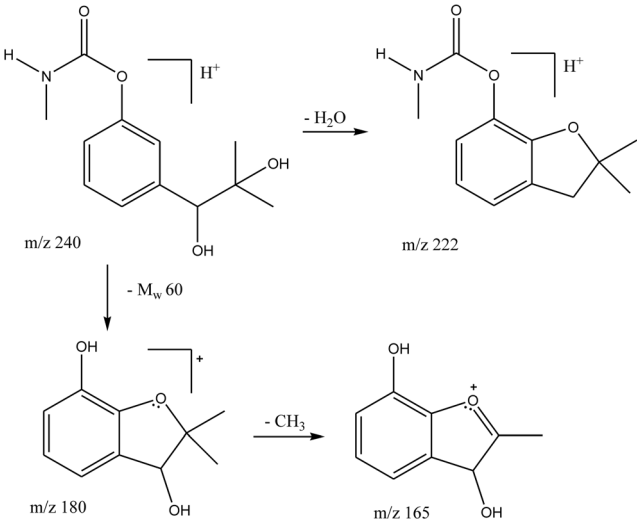

Fig. 7 Fragmentation pathways of *m*/*z* 240 ion

fragment (Mw 60) from *m*/*z* 240 ion produced 2,2-dimethyl-2,3-dihydroxybenzofuran-3,7-diol, *m*/*z* 180 ion, and subsequent demethylation produced 3,7-dihydroxy-2-methyl-2*H*-benzofuran, an ion found at *m*/*z* 165 (Fig. 7).

The second photodegradation product (ion detected at *m*/*z* 153, TP II) was obtained from carbofuran by methyl isocyanate elimination, followed by hydroxylation of benzylic hydrogen producing 2,3-dihydrobenzofuran-3,7-diol. This product appeared after 30 min of illumination, and gradual increases of TP II concentration were observed (Fig. 5e). Dehydration of *m*/*z* 153 ion produced 2,3-dihydrobenzofuran-7-ol fragment, an ion found at *m*/*z* 135 (Fig. 8). On the other side, expulsion of carbon monoxide gave protonated 2-methoxyphenol (*m*/*z* 125), which after a loss of formaldehyde produced protonated phenol (*m*/*z* 95). The third fragmentation, which takes place by elimination of vinyl alcohol, produced protonated resorcin (*m*/*z* 111).

Photodegradation pathways of carbofuran and Furadan 35-ST defined by GC-MS

Photodegradation products of carbofuran and Furadan 35-ST were also identified by the GC-MS method, which is widely used for determination of the photodegradation mechanism of carbofuran (Mahalakshmi et al. 2007; Wang and Lemley 2003). The GC-MS analysis confirmed the formation of the following three photodegradation products of pure carbofuran: *m*/*z* 164 ion ($t_R \approx 9.05$ min), which corresponds to carbofuran phenol, and two photocatalytic dimerization products, which are *m*/*z* 278 and 281 ($t_R \approx 16.18$ and 18.05 min), respectively, while only carbofuran phenol was detected as Furadan 35-ST photodegradation product. According to GC-MS data given in Table S1, the peak at *m*/*z* 164 (Fig. S5) was attributed to carbofuran phenol ion, which is the product of the cleavage of the carbamate group from the parent compound (Fig. S6). An appearance of carbofuran phenol, a photoproduct registered in literature (Katsumata et al. 2005; Mahalakshmi et al. 2007), indicated that hydroxyl radical attack on the carbamoyl group caused a breakage of ester bond and formation of methyl carbamic acid. Relevant literature also describes carbamic acid as a carbofuran photodegradation product (Katsumata et al. 2005; Mahalakshmi et al. 2007; Bachman and Patterson 1999), which undergoes degradation by producing methylamine and CO_2 (Bachman and Patterson 1999; McMurray 1992). Fragmentation of ion *m*/*z* 164 is given and explained in Supplementary material (Fig. S6).

Compounds, observed at *m*/*z* 278 and 280 (Fig. S7), were present in all studied samples with pure carbofuran from the beginning of irradiation. Possible structures of these photoproducts were proposed, as given in Fig. S7. They were probably generated by photoinduced reaction in irradiated solution which takes place by two demethylation processes of carbofuran phenol producing Mw 148 and 133 molecules in

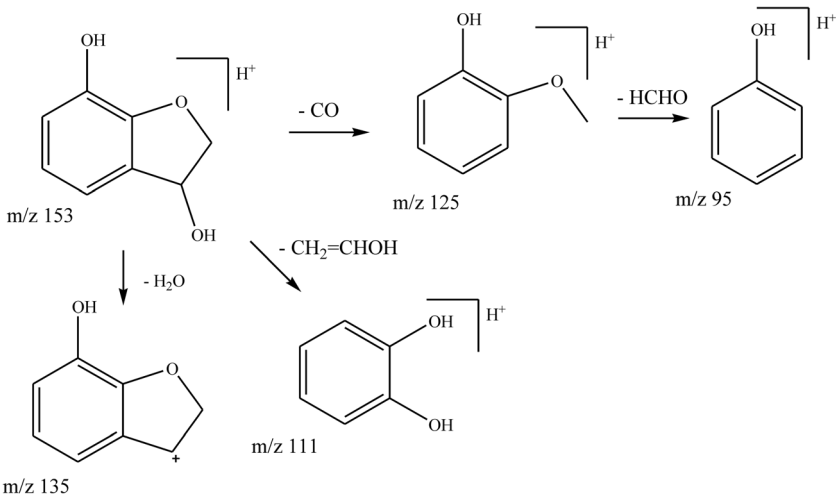

Fig. 8 Fragmentation pathways of *m*/*z* 153 ion

two consecutive steps. Hydroxyl radical attack on benzylic hydrogen generates the reactive species capable of dimerization-producing structures proposed in Fig. S7.

In summary, the presented results proved that ZnO can be a very efficient catalyst for photodegradation of carbofuran and the commercial product Furadan 35-ST. In the model system, micelles formed in the bulk and micelles on the ZnO surface influenced that the availability of carbofuran, incorporated into the mixed aggregates, is compensated by a higher carbofuran concentration at the catalyst surface. Generally, the presented methodology provides a good and applicable basis for analysis of the possible photodegradation rate/mechanism in a realistic system.

Conclusion

The influences of selected process parameters on photocatalytic degradation of carbofuran, the commercial product Furadan 35-ST, and its model formulation were studied and discussed in the presented work. The results highlight the fact that inert ingredients, present in Furadan 35-ST, have a certain influence on the photodegradation rate of the active compound. A mineralization study of both carbofuran and Furadan 35-ST, followed by IC analysis, showed an appearance of oxalate, acetate, and formate, as well as methylamine ion, $CH_3NH_3^+$. GC-MS and HPLC-MS/MS analyses confirmed the formation of the following three photodegradation products of both carbofuran and Furadan 35-ST: carbofuran phenol, 3-hydroxycarbofuran, and 3-ketocarbofuran phenol, and also the following two Furadan 35-ST degradation products: ion detected at m/z 240 (TP I) and ion detected at m/z 153 (TP II). GC-MS analysis revealed the presence of two carbofuran photocatalytic dimerization products, which are m/z 278 and 281 ($t_R \approx 16.18$ and 18.05 min). Three degradation products (ions at m/z 153, 278, and 281) had not been previously reported. Finally, the main photodegradation pathways of carbofuran leading to generation of the detected ions were proposed. The presented results of our adsorption and kinetic studies under non-competitive and competitive conditions contribute to better understanding of the photodegradation processes of active ingredients in pesticide formulations.

Acknowledgments The authors are grateful to the Ministry of Education, Science, and Technological Development of the Republic of Serbia for funding the study (Grant Nos. III46008, 172013, 172007, and TR 31043). The authors wish to thank the USA company FMC for donating the carbofuran analytical standard. The authors gratefully acknowledge Ajimoto OmniChem, Tensiofix Division, Belgium, for their recommendations, suggestions, and kindly supplied samples of surfactants.

References

Ahmed S, Rasul MG, Brown R, Hashib MA (2011) Influence of parameters on the heterogeneous photocatalytic degradation of pesticides and phenolic contaminants in wastewater: a short review. J Environ Manag 92:311–330

Arias M, García-Rio L, Mejuto JC, Rodríguez-Dafonte P, Simal-Gándara J (2005) Influence of micelles on the degradation of carbofuran. J Agric Food Chem 53:7172–7178

Bachman J, Patterson HH (1999) Photodecomposition of the carbamate pesticide carbofuran: kinetics and the influence of dissolved organic matter. Environ Sci Technol 33:874–881

Ballesteros Martín MM, Sánchez Pérez JA, García Sáanchez JL, Casas López JL, Malato Rodríguez S (2009) Effect of pesticide concentration on the degradation process by combined solar photo-Fenton and biological treatment. Water Res 43:3838–3848

Behnajady MA, Modirshahla N, Hamzavi R (2006) Kinetic study on photocatalytic degradation of C.I. Acid Yellow 23 by ZnO photocatalyst. J Hazard Mater B 133:226–232

Benicha M, Mrabet R, Azmani A (2013) Dissipation processes of ^{14}C-carbofuran in soil from northwest Marocco as influenced by soil water content, temperature and microbial activity. J Environ Chem Ecotoxicol 5:119–128

Berberidou C, Kitsiou V, Karahanidou S, Lambropoulou DA, Kouras A, Kosma CI, Albanis TA, Poulios I (2016) Photocatalytic degradation of the herbicide clopyralid: kinetics, degradation pathways and ecotoxicity evaluation. J Chem Technol Biotechnol 91:2510–2518

Bianco Prevot A, Pramauro E, de la Guardia M (1999) Photocatalytic degradation of carbaryl in aqueous TiO_2 suspensions containing surfactants. Chemosphere 39:493–502

Chowdhury MAZ, Banik S, Uddin B, Moniruzzaman M, Karim N, Gan SG (2012) Ogranophosphorus and carbamate pesticide residues detected in water samples collected from paddy and vegetable fields of the Savar and Dhamrai Upazilas in Bangladesh. Int J Environ Res Public Health 9:3318–3329

Cid AP, Andres GL, Espino MPB (2014) Challenges of a HPLC-UV analysis of methomyl, carbofuran and carbaryl in soil and fresh water for degradation studies. Int J Pharm Biol Chem Sci 3:15–22

Colina-Márquez J, Zuluaga L, Martínez FM (2009) Evaluation of the titanium dioxide photocatalysis for the degradation of a commercial pesticides mixture. Ing Des 26:156–167

Comparelli R, Fanizza E, Curri ML, Cozzoli PD, Mascolo G, Agostino A (2005) UV-induced photocatalytic degradation of azo dyes by organic-capped ZnO nanocrystals immobilized onto substrates. Appl Catal B Environ 60:1–11

Daneshvar N, Aber S, Seyed Dorraji MS, Khataee AR, Rasoulifard MH (2008) Preparation and investigation of photocatalytic properties of ZnO nanocrystals: effect of operational parameters and kinetic study. Int J Chem Biomol Eng 1:24–29

Daneshvar N, Aber S, Seyed Dorraji MS, Khataee ARM, Rasuolifard H (2007) Photocatalytic degradation of the insecticide diazinon in the presence of prepared nanocrystaline ZnO powders under irradiation of UV-C light. Sep Purif Technol 58:91–98

Daneshvar N, Salari D, Khataee AR (2003) Photocatalytic degradation of azo dye acid red 14 in water: investigation of the effect of operational parameters. J Photochem Photobiol A Chem 157:111–116

Daneshvar N, Salari D, Khataee AR (2004) Photocatalytic degradation of azo dye acid red 14 in water on ZnO as an alternative catalyst to TiO_2. J Photochem Photobiol A Chem 162:317–322

Detomaso A, Mascolo G, Lopez A (2005) Characterization of carbofuran photodegradation byproducts by liquid chromatography/hybrid quadrupole time-of-flight mass spectrometry. Rapid Commun Mass Spectrom 19:2193–2202

Environmental Protection Agency (EPA) (2006) Interim registration eligibility decision carbofuran. Washington, D.C.: Prevention,

Pesticides and Toxic Substances (7508P). U.S. Environmental Protection Agency, Report 738-R-06-031, USA.

Evgenidou E, Fytianos K, Poulios I (2005) Semiconductor-sensitized photodegradation of dichlorvos in water using TiO_2 and ZnO as catalysts. Appl Catal B Environ 59:81–89

Farahani GHN, Zakaria Z, Kuntom A, Pmar D, Ismail BS (2007) Adsorption and desorption of carbofuran in Malaysian soils. Adv Environ Biol 1:20–24

Fenoll J, Hellin P, Flores P, Martinez CM, Navarro S (2013) Degradation intermediates and reaction pathway of carbofuran in leaching water using TiO_2 and ZnO as photocatalyst under natural sunlight. J Photochem Photobiol A Chem 251:33–40

Huston PJ, Pignatello JJ (1999) Degradation of selected pesticide active ingredients and commercial formulations in water by the photo-assisted Fenton reaction. Water Res 5:1238–1246

Katagi T (2004) Photodegradation of pesticides on plant and soil surfaces. Rev Environ Contam Toxicol 182:1–195

Katsumata H, Matsuba S, Kaneco K, Suzuki T, Ohta K, Yobico Y (2005) Degradation of carbofuran in aqueous solution by Fe (III) aquacomplexes as effective photocatalyst. J Photochem Photobiol A Chem 170:239–245

Knowles A (2005) New developments in crop protection product formulation. T&F Informa, Agrow Reports, London

Knowles A (2006) New from Agrow reports—adjuvants and additives: 2006 edition. T&F Informa, London

Knowles A (2008) Recent developments of safer formulations of agrochemicals. The Environ 28:35–44

Kong L, Lemley AT (2007) Effect of nonionic surfactants on the oxidation of carbaryl by anodic Fenton treatment. Water Res 41:2794–2802

Konstantinou IK, Hela DG, Albanis TA (2004) An overview residues in surface waters of Greece during the last two decades and ecological risk assessment. 3rd European Conference on Pesticides and Related Organic Micropollutants in the Environment, Halkidiki, Greece, pp. 81–86.

Kuo WS, Chiang YH, Lai LS (2006) Degradation of carbofuran in water by solar photocatalysis in presence of photosensitizers. J Environ Sci Health Part B 4:937–948

Lhomme J, Brosillon S, Wolbert D (2008) Photocatalytic degradation of pesticides in pure water and a commercial agricultural solution on TiO_2 coated media. Chemosphere 70:381–386

Li-An L, Ying-Shih M, Mathava K, Jih-Gaw L (2011) Photochemical degradation of carbofuran and elucidation of removal mechanism. Chem Eng J 166:150–156

Lopez-Alvarez B, Tores-Palma RA, Penuela G (2011) Solar photocatalytical treatment of carbofuran at lab and pilot scale: effect of classical parameters, evaluation of the toxicity and analysis of organic by-products. J Hazard Mater 191:196–203

MacBean C (2012) The pesticide manual, sixteen ed. In: BCPC, GU34 2QD. Hampshire, Alton

Mahalakshmi M, Arabindoo B, Palanichamy M, Murugesan V (2007) Photocatalytic degradation of carbofuran using semiconductor oxides. J Hazard Mater 143:240–245

Malato S, Blanco J, Richter C, Fernández P, Maldonado MI (2000) Solar photocatalytic mineralization of commercial pesticides: oxamyl. Sol Energy Mater Sol Cells 64:1–14

Malato S, Fernandez-Ibanez P, Maldonado MI, Blanco J, Gernjak W (2009) Decontamination and disinfection of water by solar photocatalysis: recent overview and trends. Catal Today 147:1–59

Mazille F, Schoettl T, Klamerth N, Malato S, Pulgarin C (2010) Field solar degradation of pesticides and emerging water contaminants mediated by polymer films containing titanium and iron oxide with synergistic heterogeneous photocatalytic activity at neutral pH. Water Res 44:3029–3038

McMurray J (1992) Organic chemistry, third edn. Brooks/Cole Publishing, Belmont, CA

Mohammad A, Gary KCL, Ralph WM (1990) Effects of common inorganic anions on rates of photocatalytic oxidation of organic carbon over illuminated titanium dioxide. J Phys Chem 94:6820–6825

Navarro S, Fenoll J, Vela N, Ruiz E, Navarro G (2009) Photocatalytic degradation of eight pesticides in leaching water by use of ZnO under natural sunlight. J Hazard Mater 172:1303–1310

Neppolian B, Choi HC, Sakthivel S, Arabindoo B, Murugesan V (2002a) Solar/UV-induced photocatalytic degradation of three commercial textile dyes. J Hazard Mater B 89:303–317

Neppolian B, Choi HC, Sakthivel S, Arabindoo B, Murugesan V (2002b) Solar light induced and TiO_2 assisted degradation of textile dye reactive blue 4. Chemosphere 46:1173–1181

Oller I, Gernjak W, Maldonado MI, Perez-Estrada LA, Sanchez-Perez JA, Malato S (2006) Solar photocatalytic degradation of some hazardous water-soluble pesticides at pilot-plant scale. J Hazard Mater B 138:507–517

Otieno POI, Lalah JO, Virani M, Jondiko IO, Schramm K-W (2010) Soil and water contamination with carbofuran residues in agrocultural farmlands in Kenya following the application of the technical formulation Furadan. J Environ Sci Health B 45:137–144

Quiroz MA, Bandala ER, Martínez-Huitle CA (2011) Advanced oxidation processes (AOPs) for removal of pesticides from aqueous media. In: Stoytcheva M (ed) Pesticides—formulations, Effects, Fate, InTech Publishers, Rijeka, pp 687–730.

Senthilnathan J, Philip L (2010) L removal of mixed pesticides from drinking water system using surfactant-assisted nano-TiO_2. Water Air Soil Pollut 210:143–154

Sharma A, Lee B-K (2016) Rapid photo-degradation of 2-chlorophenol under visible light irradiation using cobalt oxide-loaded TiO_2/reduced graphene oxide nanocomposite from aqueous media. J Environ Manag 165:1–10

Sinha S, Orozco NGT, Ramirez DSA, Rodriguez-Vásquez R (2009) Effect of surfactant on TiO_2/UV mediated heterogeneous photocatalytic degradation of DDT in contaminated water. NSTI-Nanotech 2:411–414

Tadros TF (2005) Applied surfactants. Wiley-VCH Verlag GmbH & Co., KgaA, Weinheim

Tamimi M, Belmouden M, Qourzal S, Assabbane A, Ait-Ichou Y (2006) Photocatalytic degradation of methomyl with the presence of titanium dioxide (Degussa P-25). Fresenius Environ Bull 15:1226–1231

Tanaka FS, Wien RG, Mansager ER (1979) Effect of nonionic surfactants on the photochemistry of 3-(4-chlorophenyl)-1,1-dimethylurea in aqueous solution. J Agric Food Chem 27:774–779

Tanaka FS, Wien RG, Mansager ER (1981) Survey for surfactant effects on the photodegradation of herbicides in aqueous media. J Agric Food Chem 29:227–230

Tanaka FS, Wien RG, Zaylskie RG (1977) Photolysis of 3-(4-chlorophenyl)-1,1-dimethyurea in dilute aqueous solutions. J Agric Food Chem 25:1068–1072

Tang L, Wang J, Zeng G, Liu Y, Deng Y, Zhou Y, Tang J, Wang J, Guo Z (2016) Enhanced photocatalytic degradation of norfloxacin in aqueous Bi_2WO_6 dispersions containing nonionic surfactant under visible light irradiation. J Hazard Mater 306:295–304

Tennakone K, Tilakaratne CTK, Kottegoda IRM (1997) Photomineralization of carbofuran by TiO_2 supported catalyst. Water Res 31:1909–1912

Tomašević A (2011) Contribution to the studied of the photodegradation mechanism of carbamate pesticides. Dissertation, University of Belgrade.

Tomašević A, Bošković G, Mijin D, Đilas S, Kiss E (2007) The extremely high stability of carbofuran pesticide in acidic media. Acta Periodica Technologica 38:97–103

Tomašević AV, Gašić SM (2012) Impact of methomyl and carbofuran insecticides on environment and their remediation by photochemical processes. In: Daniels JA (ed) Advances in environmental research. Nova Science Publishers Inc., New York, pp 33–67

Tomašević A, Kiss E, Petrović S, Mijin D (2010a) Study on the photocatalytic degradation of insecticide methomyl in water. Desalination 262:228–234

Tomašević A, Mijin D, Gašić S, Kiss E (2014) The influence of polychromatic light on methomyl degradation in TiO_2 and ZnO aqueous suspension. Desalin Water Treat 52:4342–4349

Tomašević A, Mijin D, Kiss E (2010b) Photochemical behavior of the insecticide methomyl under different conditions. Sep Sci Technol 45:1617–1627

Vicente R, Soler J, Arques A, Amat AM, Frontistis Z, Xekoukoulotakis N, Mantzavinos D (2014) Comparison of different TiO_2 samples as photocatalyst for the degradation of mixture of four commercial pesticides. J Chem Technol Biotechnol 89:1259–1264

Wang Q, Lemley AT (2003) Oxidative degradation and detoxification of aqueous carbofuran by membrane anodic Fenton treatment. J Hazard Mater B 98:241–255

Wang Y, Lu K, Feng C (2013) Influence of inorganic anions and organic additives on photocatalytic degradation of methyl orange with supported polyoxometalates as photocatalyst. J Rare Earths 31:360–365

Woods TS (2003) Pesticide formulations, Encyclopedia of agrochemicals, Wiley online library, DOI 10.1002/047126363X. agr, pp 185.

Ying-Shih M, Mathava K, Jih-Gaw L (2009) Degradation of carbofuran-contaminated water by the Fenton process. J Environ Sci Health Part A 44:914–920

Zapata A, Oller I, Bizani E, Sánchez-Pérez JA, Maldonado MI, Malato S (2009a) Evaluation of operational parameters involved in solar photo-Fenton degradation of a commercial pesticide mixture. Catal Today 144:94–99

Zapata A, Velegraki T, Sánchez-Pérez JA, Mantzavinos D, Maldonado MI, Malato S (2009b) Solar photo-Fenton treatment of pesticides in water: effect of iron concentration of degradation and assessment of ecotoxicity and biodegradability. Appl Catal B Environ 88:448–454

Zhang Y, Wu H, Zhang J, Wang H, Lu W (2012) Enhanced photodegradation of pentachlorophenol by single and mixed cationic and nonionic surfactants. J Hazard Mater 221:92–99